

ANALYSIS OF TAPERED FINLINE IN POWER COMBINER FOR WIDEBAND APPLICATION

Nur Shaheera Alia Sadick, Ali Mohamad Zoinol Abidin Abd Aziz*, Badrul Hisham Ahmad, Mohd Azlishah Othman, Hamzah Asyrani Sulaiman

Centre for Telecommunication Research and Innovation (CeTRI), Faculty of Electronics and Computer Engineering, Universiti Teknikal Malaysia Melaka (UTeM), 76100 Durian Tunggal, Melaka, Malaysia

Article history

Received

14 June 2015

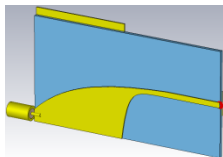
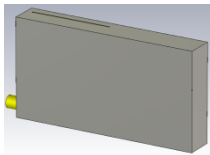
Received in revised form

14 September 2015

Accepted

14 December 2015

*Corresponding author
mohamadzoinol@utem.edu.my



Abstract

Tapered finline or slotline array has used in Vivaldi antenna design to produce Ultra-wideband (UWB). This paper focuses to design and analysis the structural of tapered finline in order to achieved wideband in rectangular waveguide power combiner at frequency 0.5 GHz to 6 GHz. There are three main parameters are studying in this paper which are of length of radiation region exponential coefficient at curves of radiation and exponential coefficient at curves of directivity. The design of tapered finline in power combiner is simulated using CST Microwave Studio Software. The simulation process is based on the input return loss at port 1 (S11), input return loss at port 2 (S22), isolation (S21) and insertion loss (S12). By studying the effect of the parameter on the design structure, it can be ensure that the tapered finline structures are suitable in wideband design.

Keywords: Tapered finline, power combiner

© 2016 Penerbit UTM Press. All rights reserved

1.0 INTRODUCTION

In wireless communication systems and particular transmitter hardware, power amplifiers (PAs) are very important. Generally, PAs for low microwave frequencies have high-performance characteristics but still limited in power and are difficult to design at higher microwave and millimeter-wave frequencies. This has encouraged a special interest in finding alternative solutions [1]. Power dividers and combiners are widely used in microwave/millimeter-wave circuits for distributing and processing signals as needed, especially in application of wideband power amplification where output power from an individual device is not enough [2]. Generally, millimeter-wave solid-state power combining can be divided into four types which are circuit-level power combining, chip-level power combining, spatial power combining and hybrid type power combining [3]. Many circuit-level

combining approaches, such as corporate combining, suffer from increased loss (and, hence, reduced combining efficiency) as the number of devices increases. On the contrary, loss is relatively independent of the number of devices in a well-designed spatial combiner. As a result, spatial power combining is preferred in certain high power applications requiring a large number of amplifiers [4]. For the implementation of high-power spatial combiners, where the output power is at the level of tens or hundreds of watts, several issues have to be incorporated in the design to achieve the desired performance. When dealing with a large number of high-power amplifiers, thermal management is extremely important since device performance degrades drastically if waste heat cannot be removed efficiently. The combiner must be compact, but large enough (physically and thermally) to accommodate the desired number of amplifiers.

Minimizing output combiner losses is also critical as far as combiner efficiency is concerned. It is worth emphasizing that for combiner systems based on high-gain amplifiers, only the loss associated with the output network is important [5]. Previous paper had reported a waveguide-based spatial power-combiner circuit that addressed these issues [6]–[8]. The concept is illustrated schematically in Figure 1 which is exploit the inherent spatial distribution of the field energy in the dominant waveguide mode to distribute and collect power to and from a dense array of amplifiers. Transitions between the amplifier and waveguide mode are made via electrically close tapered-slot antennas (or finline structures). The enclosed waveguide provides an excellent heat-sinking environment for the power devices and is a natural choice for most high-power applications [9].

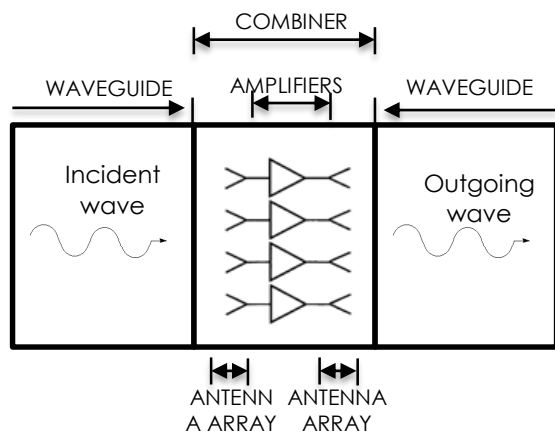


Figure 1 Schematic Diagram

2.0 POWER COMBINER

The rectangular waveguide spatial power combining structure proposed consists of tapered slot (finline structure). The rectangular waveguide used perfect electric conductor (PEC) because it is an idealized material exhibiting infinite electrical conductivity or, equivalently, zero resistivity [1]. At both ends of the waveguide, a coaxial adapter (input port) and discrete port (output port) provide a standard 50 Ohm SMA connector. In order to couple the energy travelling inside the waveguide structure, some UWB matched transitions need to be designed. Those transitions are defined in literature as “antennas”, but they are nothing but finlines inserted into the waveguide environment. The Vivaldi-like shape is able to provide a considerable wide band. In this work, exponentially-tapered finline transitions are used. The equations given in [11] for the synthesis of Vivaldi antennas can be used for a preliminary estimation of the taper parameters. The exponential profile curves employed in this structure E_a , E_b and E_c are expressed according to the following functions:

$$y = \pm [C_1 e^{Rx} + C_2] \quad [1]$$

$$C_1 = \frac{y_2 - y_1}{e^{Rx_2} - e^{Rx_1}} \quad [2]$$

$$C_2 = \frac{y_1 e^{Rx_2} - y_2 e^{Rx_1}}{e^{Rx_2} - e^{Rx_1}} \quad [3]$$

Where C_1 and C_2 are the constant, R is the the opening rate. If the two points $P1 (X_1, Y_1)$ and $P2 (X_2, Y_2)$ are supposed as the beginning and the end points, then Y indicates the distance between the exponential edge and the central axis in the direction perpendicular to the central axis, while X indicates the that between the edge and bottom of the antenna in the direction parallel to the central axis. The tapered slot (finline structure) consists of two copper layers; the bottom layer (back) is connected to the ground planes and the top layer (front) is connected to the input port of the feeding line. The thickness of copper (t) is 0.5mm. Normally, the gradient curve is symmetrical for top layer (front) and bottom layer (back). The substrate used in this design is vacuum. Vacuum has a relative permittivity of one, for air the value is slightly higher ($\epsilon_r = 1.0006$) [12] but can consider to be one for nearly all engineering applications. The geometry parameters are presented in Figure 2(a) and Figure 2(b) meanwhile Table 1 shows the dimensions: W_g , L_g and H_g are the overall width, length and height of the rectangular waveguide, W_s , L_s and h are the overall width, length and thickness of substrate. W_f and W_{ff} are the width of the strip-line and corresponding ground plane width, L_3 defines as the aperture width, L_1 is tapered length and exponential coefficient are E_a , E_b and E_c .

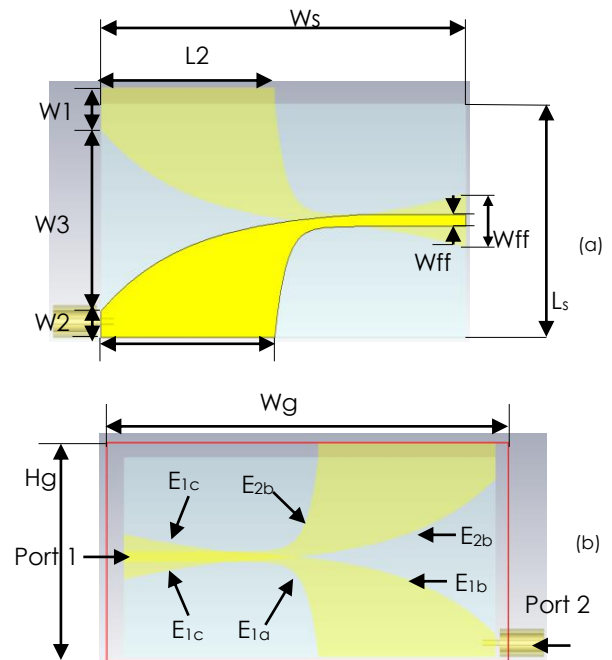


Figure 2 Power combiner, (a) front view, (b) back view

Table 1 Antenna design parameter for power combiner

Description	Design Parameter	Value (mm)
Width of waveguide	Wg	91
Height of waveguide	Hg	48
Length of waveguide	Lg	14
Width of substrate	Ws	84
Length of substrate	Ls	44
Length of radiation region top layer	$L1$	40
Length of radiation region bottom layer	$L2$	40
Width of radiation region top layer	$W1$	5
Width of radiation region bottom layer	$W2$	5
Opening width	$W3$	34
Width of feedline (top layer)	Wf	2.24
Width of feedline (bottom layer)	Wff	10
Exponential coefficient at curves of radiation (top layer)	E_{1b}	0.05
Exponential coefficient at curves of radiation (bottom layer)	E_{2b}	0.05
Exponential coefficient at curves of directivity (top layer)	E_{1a}	0.4
Exponential coefficient at curves of directivity (top layer)	E_{2a}	0.4
Exponential coefficient at feedline (bottom layer)	E_{1c}	0.15
Thickness of copper	t	0.5
Thickness of substrate	h	1.6

3.0 RESULTS AND DISCUSSION

In order to achieve high performance in the microwave region, finline structure need to design from the two aspects which are transition section and radiating section. The design of finline structure involves a lot of design parameters and the design process used parametric study to see their constantly approaching the desired result. There are three parameters could affect the performances respectively which are length of radiation region, curves of radiation and curve of directivity [13].

3.1 Length of Radiation Region

The result in Figure 3 shows the return loss for port 1, port 2, insertion loss (S12) and isolation (S21) when length of radiation region top layer ($L1$) and bottom layer ($L2$) varies. Figure 3(a) and 3(b) show result of return loss for input port (port 2) and output port (port 1). Both results have the same response. The result shows that as the length of radiation region ($L3$) changed the response have minimum altered and narrow bandwidth. There are four minimum points of return loss at S11 and three minimum points at S22. The differences changes at

frequency 5.8 GHz and the return loss for S11 is -16.354 dB and S22 is -32.347 dB. Figure 3(c) and Figure 3(d) show the result of isolation and insertion loss. There are difference responses at frequency 1 GHz to 2 GHz. The minimum insertion loss and isolation slightly same but the response a bit shifted when length of radiation region changes. When length of radiation region increase, the response will shift minimally 100 MHz.

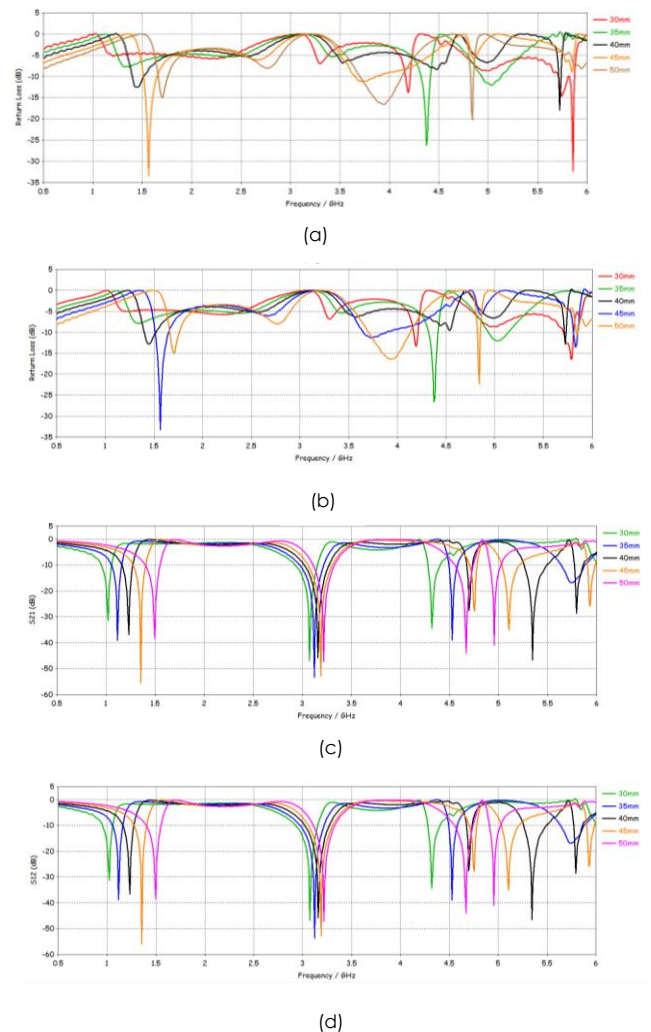


Figure 3 Parametric study of S-parameter for length of radiation region, (a) Input return Loss of Port 1 (S11), (b) Input return Loss of Port 2 (S22), (c) Isolation (S21), (d) Insertion Loss (S12)

3.2 Exponential Coefficient at Curves of Radiation

Figure 4 illustrates result for variation of exponential coefficient for top layer (E_{1b}) and bottom layer (E_{2b}) at curves of radiation for return loss at port 1 (S11), return loss at port 2 (S22), insertion loss (S12) and isolation (S21). The values of E_{1b} and E_{2b} are varying from 0.05 to 1.25. When value of E_{1b} and E_{2b} smaller, the opening width will widen and vice versa. When the slot of opening width increase, the surface current path become shorter and it will lead the resonance

point shifting to the high frequency [3]. Therefore, when the width is smaller, the structure has a better return loss in low frequency. From the parametric study, it shows that when the value of E_{1b} and E_{2b} is 0.05 it have slightly different response compare to others. This is because the curve more tapered. The minimum return loss for 0.05 is near 10 dB and minimum return loss for higher value is near 15 dB. There are one point have better return loss for both port which is -24.251 dB at 4.34 GHz. Figure 4(c) and 4(d) clearly show that the isolation and insertion loss have similar response except when the value of E_{1b} and E_{2b} is 0.05. The response for isolation and insertion loss at 3.16 GHz is approximately 1dB but the response become higher when E_{1b} and E_{2b} is 0.05 due to the deep curve and it is approximately -46 dB.

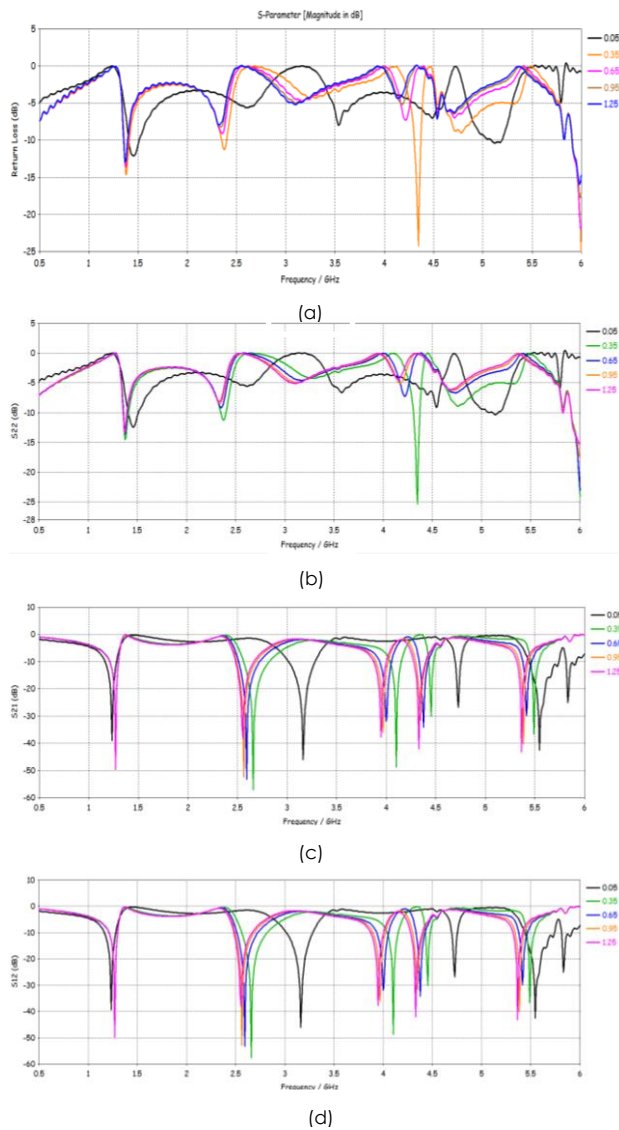


Figure 4 Parametric study of S-parameter for exponential coefficient at curves of radiation, (a) Input return Loss of Port 1 (S11), (b) Input return Loss of Port 2 (S22), (c) Isolation (S21), (d) Insertion Loss (S12)

3.3 Exponential coefficient at curves of directivity

Figure 5 illustrates result for variation of exponential coefficient top layer (E_{1a}) and bottom layer (E_{2a}) at curves of directivity for return loss at port 1 (S11), return loss at port 2 (S22), insertion loss (S12) and isolation port (S21). The value of E_{1a} and E_{2a} initially started from 0.10 to 0.70. The return loss response for port 1 and port 2 has similarity. At frequency 5 GHz to 5.5 GHz the return loss slightly different and the bandwidth increase when value of E_{1a} and E_{2a} decrease. The highest return loss is -28.694 dB and the lowest return loss is -6.32 dB. The insertion loss and isolation response slightly unchanged even the values are varied. The response have a shifted from 1 GHz to 1.5 GHz when value of E_{1a} and E_{2a} decrease. Meanwhile, the response shifted from 3 GHz to 3.5 GHz when value of E_{1a} and E_{2a} increase.

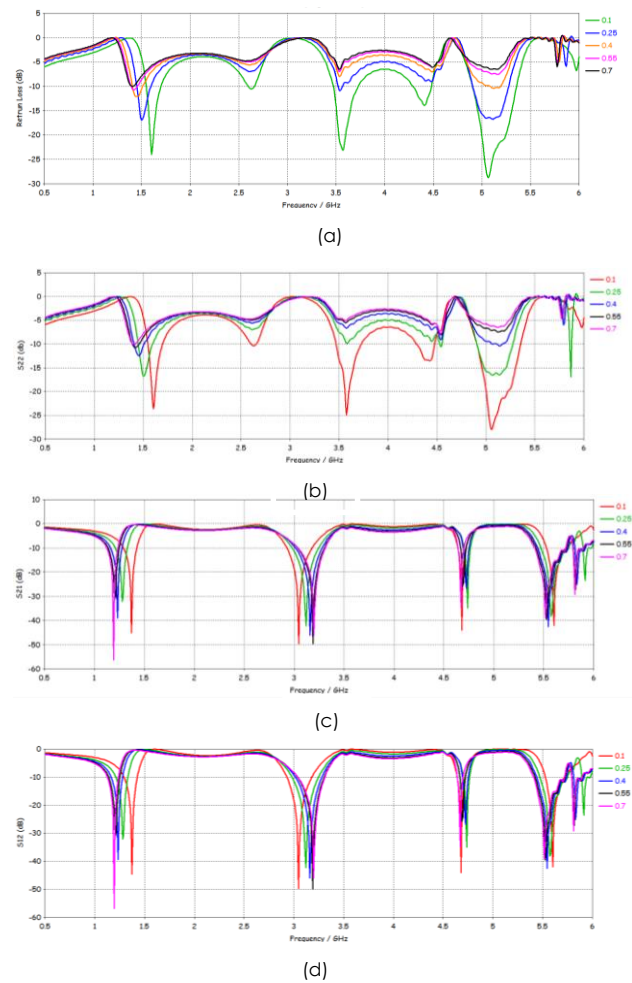


Figure 5 Parametric study of S-parameter for exponential coefficient at curves of directivity, (a) Input return Loss of Port 1 (S11), (b) Input return Loss of Port 2 (S22), (c) Isolation (S21), (d) Insertion Loss (S12)

4.0 CONCLUSION

In this paper, power combiner has been proposed and analyzed. The range of frequency used for this paper started from 0.5 GHz to 6 GHz. There are three parametric studies chosen at the finline structure which are length of radiation region, exponential coefficient at curves of radiation and exponential coefficient at curves of directivity. There will affect the changes of return loss when length of radiation region and exponential coefficient at curves of radiation varies. Meanwhile, the changes of exponential coefficient at curves of directivity will increase the bandwidth region. For future study, this design could be fabricated and the measurement result can be used to do comparison with the simulation result.

Acknowledgement

The authors would like to thank to Universiti Teknikal Malaysia Melaka (UTeM) for supporting in obtained the information and material in the development for our work. We also thank the anonymous referees whose comments led to an improved presentation of our work.

References

- [1] Belai, M. and Wu, K. 2003. Spatial Power Amplifier Using a Passive and Active TEM Waveguide Concept. *IEEE Transactions on Microwave Theory and Techniques*.
- [2] Zhang, Lei, Zhu, Xiaowei, and Zhai, Jianfeng. 2012. Design of Wideband Planar Power Dividers/Combiners. *IEEE MTT-S International Microwave Workshop Series on Millimeter Wave Wireless Technology and Applications, IMWS*.
- [3] Chen, Mingyong and Dou, Wenbin. 2009. A W-band Quasi-Optical Power Combiner Based on Waveguide Lens. *IEEE Transactions on Microwave Theory and Techniques*.
- [4] Cheng, N. S., Alexanian, A., Case, M. G., and York, R. A. 1998. 20-W Spatial Power Combiner in Waveguide. *IEEE MTT-S Int. Microwave Symp. Dig.*
- [5] N.-S. Cheng, A. Alexanian, M. G. Case, and R. A. York. 1998. 20-W Spatial Power Combiner in Waveguide. *IEEE MTT-S Int. Microwave Symp. Dig.*
- [6] Alexanian, A. and York, R. A. 1997. Broad-Band Waveguide-Based Spatial Combiner. *IEEE MTT-S Int. Microwave Symp. Dig.*
- [7] 1997. Broad-Band Spatially Combined Amplifier Array Using Tapered Slot Transitions In Waveguide. *IEEE Microwave Guided Wave Lett.* 7: 42-44.
- [8] 1998. *Waveguide-Based Spatial Power Combining Array And Method For Using The Same*. U.S. Patent 5 736 908.
- [9] Chen, Nai-Shuo, Case, A. A. M. G. Rensch, D. B., and York, R. A. 1999. 40-W CW Broad-Band Spatial Power Combiner Using Dense Finline Arrays. *IEEE Transactions On Microwave Theory And Techniques*. 47.
- [10] Henyey, F. S. 1982. Distinction between a Perfect Conductor and a Superconductor. *Phys. Rev. Lett.* 49.
- [11] Peng F., Jiao Y.-C., Hu, W., Zhang F.-S. 2011. A Miniaturized Antipodal Vivaldi Antenna with Improved Radiation Characteristics. *IEEE Antennas and Wireless Propagation Letters*. 10: 127-130.
- [12] Bakshi U. A., Bakshi A. V. 2010. *Element of Electrical Engineering*. 2-9.
- [13] Yang, L., Guo, H., and Liu, X. 2010. An Antipodal Vivaldi Antenna for Ultra-Wideband System. *IEEE International Conference on Ultra-Wideband, ICUWB2010*.